Research Open

Geology, Earth and Marine Sciences
Volume 6 Issue 6

Research Paper

The Formation of Some Quartz Veins in the Lusatian Massif, E-Germany by Supercritical Fluids/Melts Bearing Lonsdaleite and Diamond and Comparison with Other Similar Formations in Middle-Saxonian and Thuringian/E-Germany

Rainer Thomas[1]* and Michael Leh[2]

[1]Im Waldwinkel 8, D-14662 Friesack, Germany
[2]Neuer Weg 6, D-02699 Neschwitz, Germany

Corresponding author: Thomas, Im Waldwinkel 8, D-14662 Friesack, Germany

Received: September 19, 2024; **Accepted:** September 24, 2024; **Published:** September 30, 2024

Abstract

In this paper, we show that quartz veins in the Lusatian Massif were primarily generated by supercritical fluids coming from mantle deeps, rising very fast into the crust region. For the substantiation of our conclusions, we use the occurrence of lonsdaleite and microdiamonds in the root zones of quartz crystals from these quartz veins. Hydrothermal fluids afterward reworked the so primarily formed veins in more than one step. This hydrothermal activity hides the primary origin of the veins. For corroboration of the proofs, we used other examples from the Saxon Granulite Massiv, the Central Erzgebirge, and E-Thuringia.

Keywords: *Lusatian Massif, Quartz veins, Lonsdaleite, Diamond, Raman spectroscopy*

Introduction

In a row of publications, the author and co-authors [1-8] have used melt inclusions to the characterization of the pegmatite-forming melt and the high-temperature quartz veins in the Lusatian massif. Primarily, these studies focused on single aspects of new minerals in this region and the formation of respective geological objects. That also includes the determination of pseudo-binary solvus curves and some element enrichment related to such curves, which often show a Lorentzian distribution [2,3,7,8]. In this contribution, we will show that all studied objects clearly indicate that supercritical fluids or melts trigger the cause of the formation of those apparent and different objects (granites, pegmatites, and quartz veins). The first indications came from the high-speed intrusion velocity of the Königshainer granite melt [5], with about 700 to 1000 m/year. Later, this value increased significantly because larger magmatic epidote crystals could be found. Up to this point, there was a relationship between granite-forming melt and the formation of quartz veins and supercritical fluids or melts already not given. However, the similarities of the solvus curves of all studied objects were a solid hint of a uniform process. In addition, the Lorentzian distribution of some main and trace elements around the solvus crest demands a process of overriding importance. The finding of diamond and water-rich stishovite in a different geological unit, the Saxonian Granulite Massif, opened the eyes to processes that were not important up to now [8,9]. An earlier paper showed Thomas et al. (2020) [10] on the example of emeralds from the Habachtal that the new results of melt inclusions in this mineral generated a conflict with the accepted geological model. With the acceptance of supercritical fluids, this conflict is soluble. Here, we will show that the formation of the granite stock from Königshainer and a large part of quartz veins in the Lusatian region are influenced or generated by supercritical fluids or melts coming from mantle depths.

Sample Material and Earlier Results

Details of the used sample material are in the references above. A short explanation is necessary for the quartz samples from Lauba. For the preparation (grinding and polishing) of quartz thick sections (500 µm thick), diamond was not used. For polishing this quartz, we used a suspension of silica in a ten percent KOH solution using the Speed Fam of the Danish company Haldor Topsøe. From both sides, 100 µm were removed. Generally, we tried to remove all diamond rests from all used samples, which may have been induced by grinding and polishing (see results and discussion in Thomas et al., 2023) [9] using an ultrasound bath. A large number of quartz veins in the Lusatian Massif were described by Bartnik (1969) [11]. By an extensive effort, we could only study a minimal number of samples. For the selection of usable samples, the root zone must contain melt inclusions because diamonds, etc., are present only in these zones. The water-clear parts of the quartz crystals do not include such minerals. These are formed by later activation and recrystallization.

The following samples are studied:

1. Quartz from the Königshainer granite [4,5]
2. Quartz crystals from Sproitz [12].
3. Quart crystal from Caminau [13]
4. Quartz crystals from Lauba [13]
5. Quartz crystals from Oppach [2,3,6].
6. Quartz crystals from Steinigwolmsdorf [7,16].
7. Massif blue quartz with a brownish coat at fissures from Berthelsdorf near Neustadt W-Lusatian [14].

Figure 1: A typical quartz crystal from Steinigtwolmsdorf/Lusatia [16].

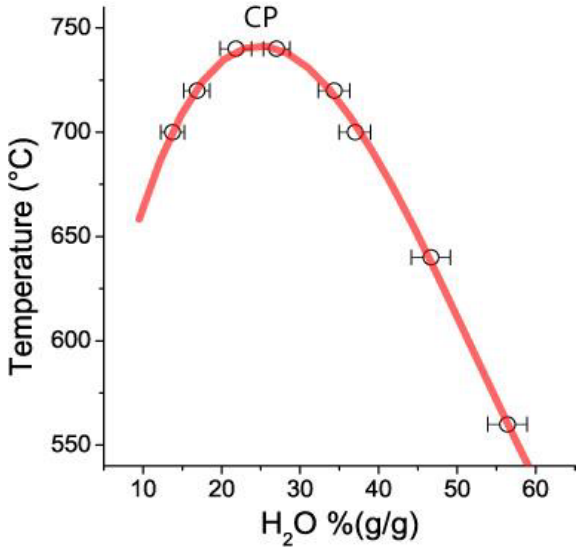

Figure 2: Pseudo-binary solvus curve (Temperatur vs. water concentration) derived from re-homogenized melt inclusions in quartz from Steinigtwolmsdorf/Lusatia. CP is the critical point (740°C, ~4.5 kbar, 27% H_2O). It is very typical for such solvus curves that the distribution of some principal and trace elements obey a Lorentzian curve, like Figure 3, the distribution of NaCl and $CaCl_2$ versus water concentration.

Unusual in sample 7 is the abundance of graphite (Raman band: 1579.4 ± 3.0, FWHM = 21,5 ± 6.4 (FWHM – Full-Width at Half Maximum) and the occurrence of tiny crystals of thortveitite (R061065, 97% Match, see Lavuente et al., 2016) [15].

In the root zone, there are many melt inclusions. Rehomogenization at different temperatures and pressures of ~4.5 kbar and the following determination of the water concentration in the melt inclusions give a pseudo-binary solvus curve (Figure 2).

What we see from Figure 3 is that Na and Ca behave reciprocally. That means that at or near the critical point of a solvus curve, a

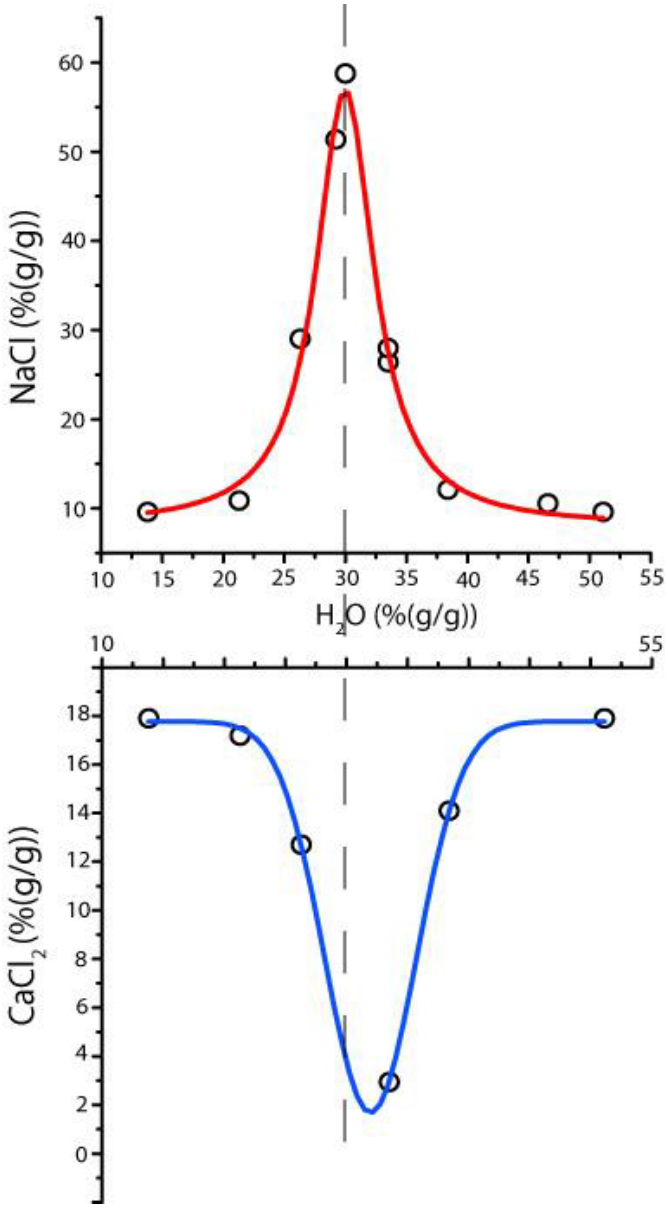

Figure 3: Schematic Lorentzian distributions of NaCl and $CaCl_2$ in melt inclusions from Steinigtwolmsdorf/Lusatia in dependence on the water content. The plot is highly schematic because the determination of NaCl and $CaCl_2$ in highly complex fluid systems is not adequately known.

strong separation of elements, maybe also isotopes, is probably. That would be a pleasant and new research theme for the future. Like the NaCl distribution in Figure 3, we found similar distributions in many examples (Thomas et al. 2019a and 2022a) [8]. For Oppach, extremely high sulfate concentrations are typical (for example, 21.3 % SO_4) – see Thomas 2024a) [17]. The opening of a solvus curve around the critical point starts with a singularity [18]. The solvus and the Lorentzian distribution of elements around the critical point is after that authors a strong proof of supercritical transition to critical and under-critical conditions. The evidence of lonsdaleite and diamond from the mantle deep in rocks and minerals in the upper crust underlines the existence of supercritical fluids that transport material from the mantle deep into the crust. Therefore, the finding of lonsdaleite and diamond as inclusions in rocks and quartz of widespread quartz veins in the Lusatian Massif generates a new approach.

Phenotypes of Lonsdaleite and Diamond in More Crustal Rocks and Quartz Veins

Here, we will show exemplarily some lonsdaleite and diamond crystals that occur in minerals of untypical crust positions (Figures 4-6).

The formula given in Figure 6 is the ideal chemistry. According to Antony et al. (2003) [19], it is the more real formula (Ce, La)(CO_3)(OH, F) (see Lafuente et al. 2016 – [15]: RRUFF R060283). According to Kirillov (1964) [20], hydroxylbasnäsite-Ce is typically a late phase of the hydrothermal stage formed by the dissolution and reprecipitation of earlier carbonatite minerals. The main Raman band of lonsdaleite shown in Figure 6 is 1318.7 ± 4.6 cm^{-1}. This example demonstrates a maybe late formation of lonsdaleite. Some needles are even bent. Often, lonsdaleite forms prismatic crystals or whiskers [2,3]. A reference spectrum for natural lonsdaleite (Kumdykol diamond deposit, North Kazakhstan) is given by Shumilova et al., 2011 [21]. According to Németh et al. (2014) [22], lonsdaleite does not exist as discrete crystals. In this contribution, we cannot resolve

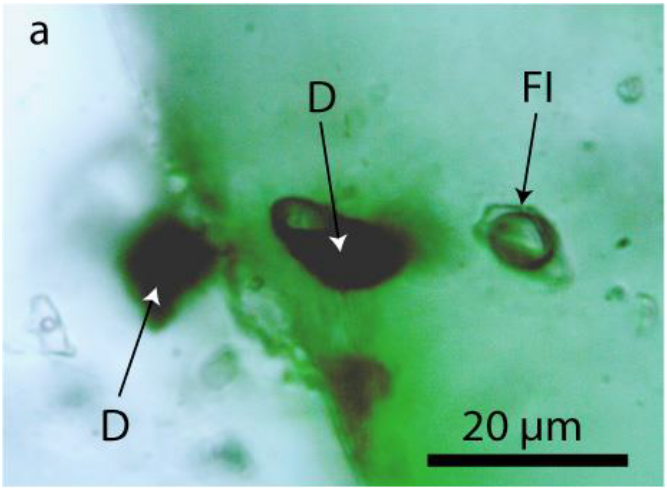

Figure 4: Diamond (D) in blue quartz from Berthelsdorf near Neustadt, W-Lusatian. The rounded light brown diamond grain is about 20 µm deep. The fluid inclusion right beside the diamond demonstrates that the hydrothermal recrystallization of the quartz did not affect the diamond. Fl: fluid inclusion

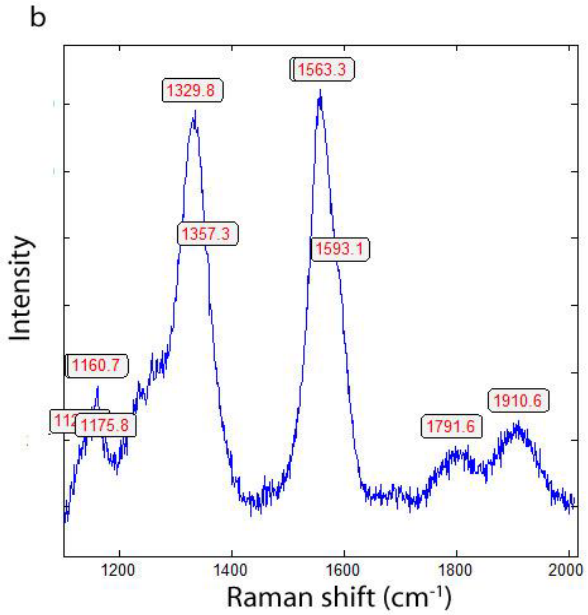

Figure 5: Raman spectrum of the rounded diamond inclusion in blue quartz from Berthelsdorf near Neustadt, W-Lusatian. The diamond inclusion is 20 µm deep under the surface.

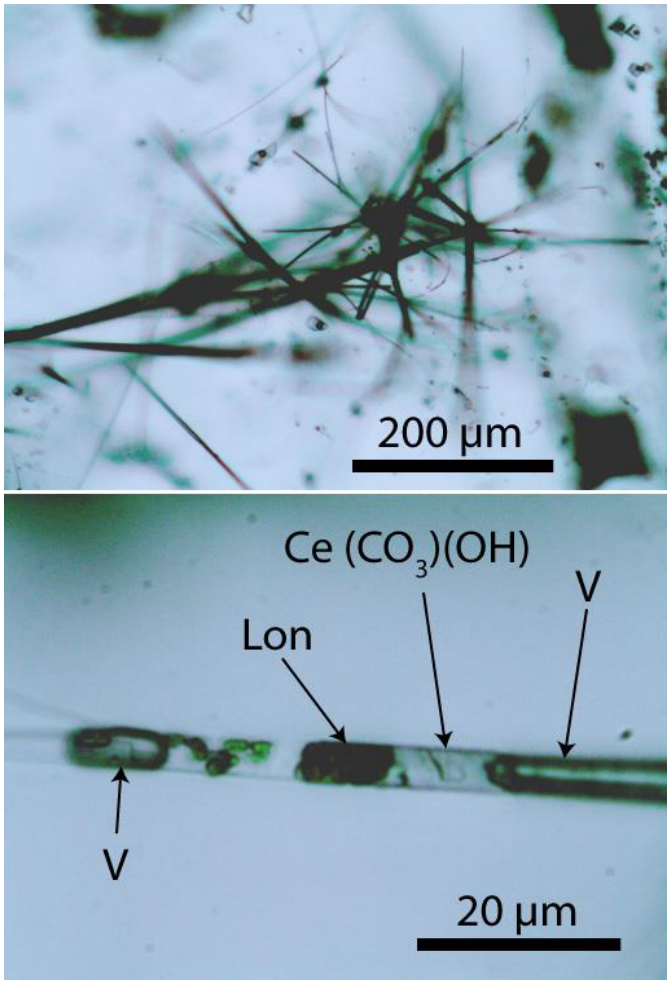

Figure 6: Needles in the root zone of quartz from Caminau near Königswartha, Lusatian Massif. The upper photomicrograph shows a jumble of needles in quartz composed of lonsdaleite (Lon) and hydroxylbasnäsite-Ce [Ce(CO_3)(OH)] and vapor. The lower photomicrograph shows details of such a needle. The needle is deep enough (45 µm) to form by contamination. V: vapor phase

this question because we only use Raman spectroscopy. However, some observations speak for the existence of lonsdaleite as whisker-like crystals [3; Figure 7].

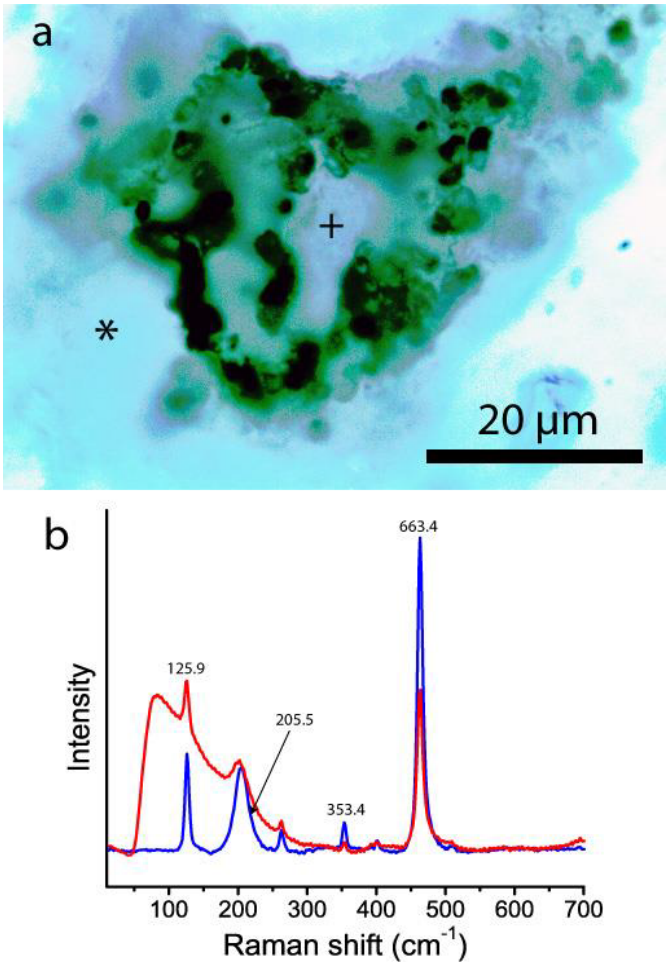

Figure 7: The microphotography a) shows an older, more gray quartz cluster (marked with "+") from Sproitz with diamond, lonsdaleite, and graphite (black) in hydrothermal quartz (marked with "∗"). The Raman spectra (b) show the differences between the two quartz generations: red, which is an older quartz, and blue, which is hydrothermal quartz.

Figure 7 shows an isolated quartz cluster with lonsdaleite, diamond, and graphite in the root zone of a quartz crystal from Sproitz (sample SP3) from the N-slope of the Gemeindberg in the rural district Görlitz/Lusatian Massif [12]. The quartz cluster shows a different Raman spectrum (red) in contrast to the matrix quartz (blue spectrum). Firstly, this quartz cluster was primarily a different SiO_2-polymorph formed at high pressure (coesite?). For comparison, we have also included the results on different rocks from Middle-Saxonian and Thuringian/E-Germany (see Table 2 and Figure 8) as well as Thomas and Recknagel 20024, Thomas and Trinkler 2024 [2,3]. Figure 8 shows an example of diamond-bearing perovskite in the granulite rock from Waldheim/Saxony (see also 2022b) [23]. The prismatic form of the diamonds is unusual. Maybe lonsdaleite was the precursor of this diamond.

The occurrence of perovskite inclusion in diamonds indicates, according to Nestola et al. (2018) [24], the recycling of oceanic crust into the lower mantle. Looking at Figure 8 raises the question of the reverse: come the diamond embedded in perovskite, saved by rutile,

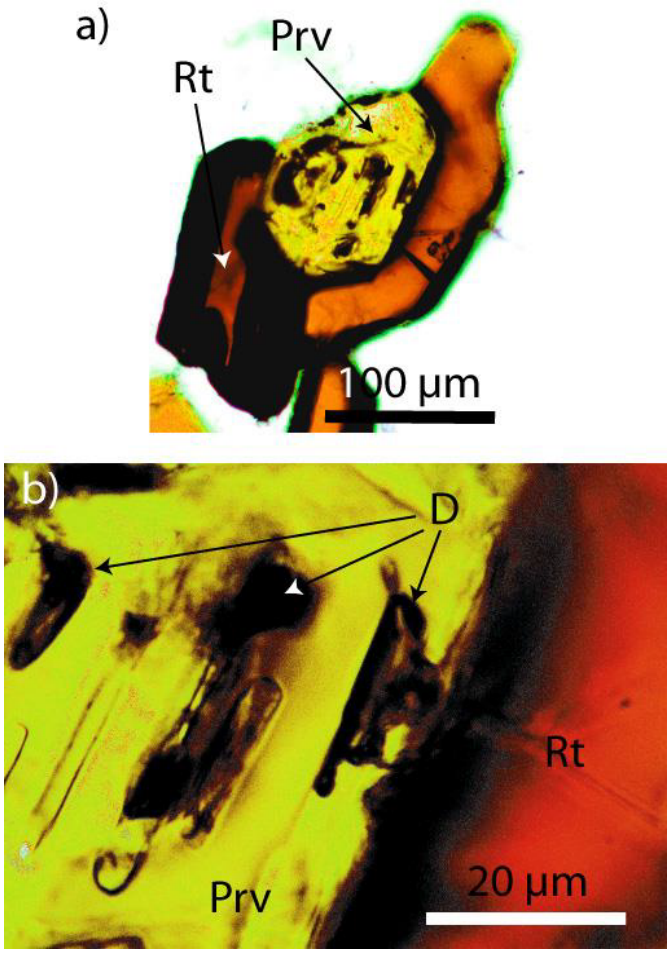

Figure 8: Diamond (D) in perovskite (Prv) [$CaTiO_3$] embedded in rutile (Rt) as foreign mineral inclusion in the prismatine rock from Waldheim/Saxony, E-Germany.

also from the lower mantle? The first finding of H_2O-rich stishovite (7.5 GPa at 1000°C, corresponding to a depth of 230 km) in the same rock [8] speaks for it.

Methodology

The techniques used (microscopy, homogenization measurements on melt inclusions, Raman spectroscopy, and electron microprobe) are described in the references above. Because Raman spectroscopy is crucial in this study, we will give more details here.

Raman Spectroscopy

Primary for the first identification of the mineral inclusion in quartz, we used for all microscopic and Raman spectrometric studies a petrographic polarization microscope with a rotating stage coupled with the RamMics R532 Raman spectrometer working in the spectral range of 0-4000 cm^{-1} using a 50 mW single mode 532nm laser. Details are in Thomas et al., 2022 and 2023 [18]. For the Raman spectroscopic routine measurements, we used the Olympus long-distance LMPLN100x as a 100x objective. We carefully cleaned the samples to delete diamond contaminations due to the preparation. For the Raman determination, we used only 20 or more µm deep crystals from the sample surface [18]. The laser energy on the sample is adjustable down to 0.02 mW. The Raman band positions were

calibrated before and after each series of measurements using the Si band of a semiconductor-grade silicon single-crystal. The run-to-run repeatability of the line position (based on 20 measurements each) was ±0.3 cm^{-1} for Si (520.4 ± 0.3 cm^{-1}) and 0.5 cm^{-1} for diamond (1332.3 ± 0.5 cm^{-1} over the range of 50–4000 cm^{-1}). We used a natural diamond crystal as a reference (for more information, see Thomas et al., 2022b) [23]. Only crystals under the surface should be measured to prevent diamond contaminations introduced by preparation (grinding, polishing). If the lonsdaleite and diamonds have needle- and whisker-like or other forms (disk-like, spherical crystals with very smooth surface, spherical sector), then the mistake is strongly reduced. We do not heat the quartz samples for homogenization of the present melt inclusions to prevent the lonsdaleite and diamonds from extensive transformation into graphite.

Results

Raman Data

First, we will show that diamonds are present in all studied quartz samples that contain a root zone. In the more or less water-clear part of the quartz crystals, we have never found lonsdaleite and diamond. We have found a general evolutionary development: lonsdaleite → lonsdaleite + diamond → diamond → nano-diamond + graphite → graphite (or, more generally, carboniferous material). Each lonsdaleite or diamond phase shows more or less a strong graphite band. A Raman spectrum of lonsdaleite is shown in Figure 9. Table 1 shows the results of our studies on lonsdaleite and diamond crystals, mostly in quartz from the Lusatian Massif. For comparison, results for the Middle-Saxonian and Thuringian regions are in Table 2.

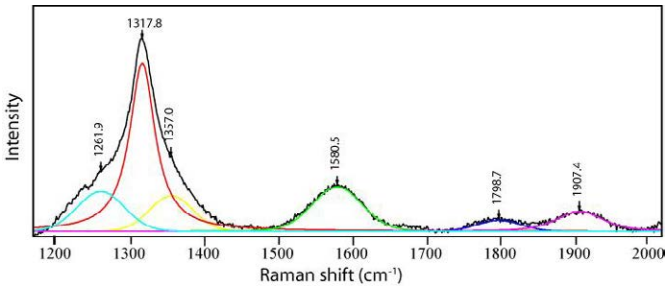

Figure 9: Raman spectrum of lonsdaleite in quartz from Steinigtwolmsdorf/Lusatia (Raman band at 1317.8 cm^{-1}, FWHM = 31.9 cm^{-1}, Raman mode: A_{1g} – see Wu 2007) – [25].

Remark

Some needles in the quartz from Caminau contain long and small lonsdaleite crystal sections with Raman bands between 1311.8 and 1313.0 cm^{-1} (Raman mode A_{1g}), corresponding, according to Wu (2007) [25] to the 2H polytype of diamond (data not in Table 1), similar to the Raman spectrum in Figure 9.

From both tables, we obtain for the lonsdaleite and diamond three groups (I: lonsdaleite, II: diamond, III: diamond under mechanical stress [26]:

I. 1320.6 ± 2.3 cm^{-1} FWHM = 65.7 ± 22.8 cm^{-1} n = 85

II. 1331.0 ± 1.9 cm^{-1} FWHM = 68.6 ± 13.4 cm^{-1} n = 121

III. 1338.8 ± 1.2 cm^{-1} EWHM = 52.4 ± 15.8 cm^{-1} n = 38

n is the number of measured lonsdaleite and diamond crystals.

All studied lonsdaleite and diamond crystals show one or two graphite-like solid G- and D2 bands of carbonaceous material [26,27]. Figure 10 shows the frequency distribution of the G-band for lonsdaleite and diamond.

The Gaussian distribution data of the G-band position (Figure 10) for lonsdaleite and diamond are in Table 3, and the data for the corresponding FWHM are in Figure 11 and Table 4. According to Frezzotti (2019) [28], the Raman analyses show clear evidence that nano-sized diamonds and, obviously, also the lonsdaleite crystals show hybrid structures, consisting of nano-diamond and -lonsdaleite

Table 1: Raman spectrometric determined the main lines of lonsdaleite and diamond in the Königshainer granite and some quartz veins in the Lusatian Massif.

Location	Mineral	Host	Raman band (cm^{-1}) ± 1σ	FWHM (cm^{-1})	Number of grains
Königshain	Lonsdaleite	Feldspar	1317.6 ± 4.5	98.0 ± 2.3	5
	Diamond	Feldspar	1331.7 ± 3.5	97.3 ± 4.4	6
	Diamond	Zircon	1336.7 ± 4.9	75.9 ± 17.7	9
Sproitz SP3	Lonsdaleite	Quartz	1319.0 ± 2.7	43.2 ± 7.2	3
	Diamond	Quartz	1333.7 ± 5.3	60.6 ± 24.4	8
Caminau	Lonsdaleite	Quartz	1318.7 ± 4.6	36.8 ± 1.5	6
	Diamond	Quartz	1332.2 ± 3.4	53.9 ± 7.1	13
Lauba	Lonsdaleite	Quartz	1316.5 ± 1.1	9.6	3
	Diamond	Quartz	1327.5 ± 5.2	45.9 ± 29.3	6
Oppach	Lonsdaleite	Quartz	1316.5	56.7	1
	Diamond	Quartz	1329.6 ± 4.7	75.1 ± 9.0	10
Steinigtwolmsdorf	Lonsdaleite	Quartz	1317.2 ± 0.4	31.3 ± 2.2	5
	Diamond	Quartz	1331.2 ± 5.0	50.9 ± 11.0	6
Berthelsdorf bei Neustadt	Diamond	Blue-Quartz	1331.8 ± 3.8	64.9 ± 14.3	14

FWHM: Full-Width at Half Maximum.

Table 2: Comparision of lonsdaleite and diamond related to supercritical fluids or melts in Middle-Saxonian and Thuringian occurrences.

Location	Mineral	Host	Raman band (cm^{-1}) ± 1σ	FWHM (cm^{-1})	Number of grains
Waldheim, Saxonia	Lonsdaleite	Zircon, Rutile	1320.4 ± 3.4	74.8 ± 8.8	7
	Diamond	Zircon, Rutile	1331.5 ± 3.5	78.3 ± 10.7	22
	Diamond	Zircon	1336.7 ± 4.9	75.9 ± 17.7	9
	Diamond	Perovskite	1331.8 ± 1.2	65.6 ± 8.1	10
Greifenstein granite	Diamond	Beryl	1328.6 ± 5.6	~60	14
	Diamond	Quartz	1333.7 ± 5.3	60.6 ± 24.4	8
Ehrenfriedersdorf	Lonsdaleite	Quarz	1318.6	100	1
	Diamond	Quartz	1331.5	46.0	1
Annaberg granite	Diamond	Quartz	1339.4 ± 12.1	41.8 ± 12.0	20
Zinnwald	Lonsdaleite	Fluorite	1318.0 ± 3.8	9.6	3
Sadisdorf	Diamond	Fluorite	1331.8 ± 5.2	83.1 ± 13.9	11
	Lonsdaleite	Fluorite	1316.5		5
Cunsdorf, Thuringia	Lonsdaleite	Quartz	1322.2 ± 1.31	75.6 ±10.9	47
	Diamond	Quartz	1329.6 ± 4.7	71.6 ± 28.8	10

FWHM: Full-Width at Half Maximum.

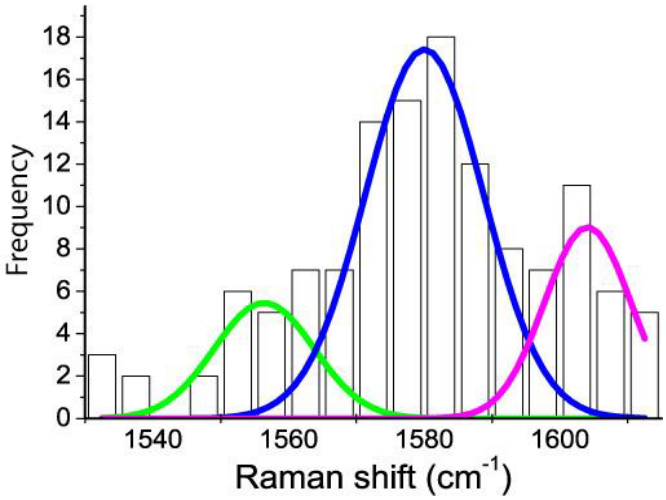

Figure 10: Frequency distribution of the G-band for lonsdaleite and diamond.

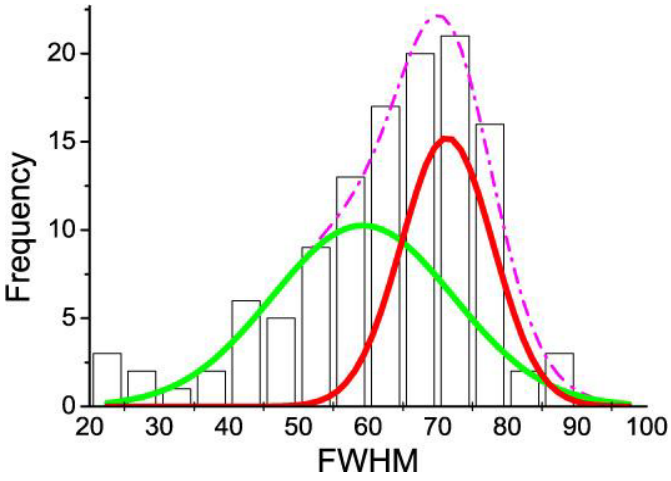

Figure 11: Frequency distribution of the FWHM for the G-bands for lonsdaleite and diamond (r^2 = 0.95066).

Table 3: Gaussian data of the G band for lonsdaleite and diamond (r^2=0.91774).

Raman band	Area	Center (cm^{-1})	Width (cm^{-1})	Height
1 (green)	100.29	1556.4	14.65	5.46
2 (blue)	380.86	1580.0	17.44	17.42
3 (magenta)	114.11	1604.1	12.73	9.03

Table 4: Gaussian distribution data for the FWHM of both components (green and red) for lonsdaleite and diamond found in crustal rocks (granite, granulite) and minerals (fluorite, quartz, perovskite, and zircon).

Raman band	Area	Center (cm^{-1})	Width (cm^{-1})	Height
1 (green)	334.81	59.23	26.04	10.26
2 (red)	251.25	71.35	13.16	15.23

and carbon groups indicated by the mostly present G-bands assigned to C=C stretching vibrations E_{2g} of graphite [29].

Discussion

The proof of lonsdaleite and diamond in crustal surroundings, together with the excellent solvus curves constructed from melt inclusions and the Lorentzian distribution of some elements, are strong proofs of supercritical fluids coming very fast from mantle deeps, bringing microcrystals of lonsdaleite and diamond as load into the crust region. The finding of these minerals in the root zones of quartz veins in the Lusatian Massif demonstrates straightforwardly that the quartz veins primarily start with the intrusion of supercritical fluids, maybe of the Variscan age, carrying lonsdaleite and diamond. Later, these early primary quartz veins are multistage reworked at lower temperatures by intensive hydrothermal activity. Through this activity, a lot of proof of the primary origin is destroyed. Only by a very intense search can such remnants be found. Meinel (2022) [30] discusses intensively the genesis of diamonds by very high volatile internal pressure in closed systems in relatively low deeps. Thomas

and co-authors [2,3,7,8,18] have shown that supercritical fluids/melts are detectable in the whole region between Lusatia, East- and Middle Erzgebirge, N-Bohemia [31] and E-Thuringia and someplace else (for example emerald deposit in the Habachtal, Austria [10]. Sometimes, however, lonsdaleite and diamond occur as needle and whisker-like crystals instead of smooth spherical microcrystals transported by supercritical fluids or melts. The same results were obtained for moissanite whiskers in beryl from Ehrenfriedersdorf (2023b) [32]. That must be an in situ formation at the upper crust. Therefore, the question result: Is the coincidence of supercritical fluids or melts with cooler upper crust granites an excellent localization for outstanding processes: solvus formation, extraordinary element enrichment in the form of the Lorentzian distribution, speedy changes of the viscosity and diffusivity of the supercritical fluids to near- and under critical conditions? This question opens new points of view for future research.

Acknowledgments

We dedicate this paper to Prof. Hans Jürgen Rösler (1920-2009), Prof. Otto Leeder (1933-2014), both from the Mining Academy Freiberg, and Dr. Günter Meinel (1933-2012) from Jena.

References

1. Thomas R (2023a) The Königshainer granite: Diamond inclusions in zircon. *Geol Earth Mar Sci* 5: 1-4.
2. Thomas R, Recknagel U (2024) Lonsdaleite, diamond, and graphite in a lamprophyre: Minette from East-Thuringia/Germany. *Geol Earth Mar Sci* 6: 1-4.
3. Thomas R, Trinkler M (2024) Monocrystalline lonsdaleite in REE-rich fluorite from Sadisdorf and Zinnwald/E-Erzgebirge, Germany. *Geol Earth Mar Sci* 6: 1-5.
4. Thomas R, Davidson P, Rhede D, Leh M (2009) The miarolitic pegmatites from the Königshain: a contribution to understanding the genesis of pegmatites. *Contrib Mineral Petrol* 157: 505-523.
5. Thomas R, Davidson P (2016) Origin of miarolitic pegmatites in the Königshain granite/Lusatia. *Lithos*. 260: 225-241.
6. Thomas R, Davidson P (2017) Hingganite-(Y) from a small aplite vein in granodiorite from Oppach, Lusatian Mts. *Mineralogy and Petrology*. 111: 821-826.
7. Thomas R, Davidson P, Appel K (2019) The enhanced element enrichment in the supercritical states of granite–pegmatite systems. *Acta Geochim* 38: 335-349.
8. Thomas R, Davidson P, Rericha A, Voznyak D (2022a) Water-Rich Melt Inclusion as "Frozen" Samples of the Supercritical State in Granites and Pegmatites Reveal Extreme Element Enrichment Resulting Under Non-Equilibrium Conditions. *Miner J* 44: 3-15.
9. Thomas R, Davidson P, Rericha A, Recknagel U (2023) Ultrahigh-pressure mineral inclusions in a crustal granite: Evidence for a novel transcrustal transport mechanism. *Geosciences*. 94: 1-13.
10. Thomas R, Davidson P, Rericha A (2020) Emerald from the Habachtal: new observations. *Mineralogy and Petrology*. 114: 161-173.
11. Bartnik D (1969) Die Quarzgänge im Lausitzer Massiv. *Geologie* 18: 21-40.
12. Schwarz D, Tietz O, Rogalla O, Rosch F (2015). Ein Quarzgang am Gemeindeberg von Kollm in der Oberlausitz. Berichte der Naturwissenschaftlichen Gesellschaft der Oberlausitz. 23: 139-150.
13. Lange W, Tischendorf G, Krause U (2004) Minerale der Oberlausitz. Verlag G. Oettel. Pg: 258.
14. Witzke T, Giesler T (2011). Neufunde und Neubestimmungen aus der Lausitz (Sachsen), Part 3. Aufschluss 62.
15. Lafuente B. Downs RT, Yang H, Stone N (2016) The power of databases: The RRUFF project. In Highlights in Mineralogical Crystallography; Armbruster T, Danisi RM, Eds.; De Gruyter: Berlin, Germany; München, Germany; Boston, MA, USA: 1–30. ISBN 9783110417104.
16. Thomas R, Davidson P, Rericha A, Tietz O (2019b) Eine außergewöhnliche Einschlussparagenese im Quartz von Steinigtwolmsdorf/Oberlausitz. Berichte der Naturwissenschaftlichen Gesellschaft der Oberlausitz. 27: 161-172.
17. Thomas R (2024a) Melt inclusions in an aplite vein in granodiorite of the Lusatian Massif: Extreme alkali sulfate enrichment. *Geol Earth Mar Sci*. 6: 1-5.
18. Thomas R, Rericha A (2023) The function of supercritical fluids for the solvus formation and enrichment of critical elements. *Geol Earth Mar Sci* 5: 1-4.
19. Anthony JW, Bideaux RA, Bladh KW, Nichols MC (2003) Handbook of Mineralogy, Vol. 5. Mineral Data Publishing, Tucson, Arizona. Pg: 813.
20. Kirillov AS (1964) Hydroxyl bastnäsite, a new variety og bastnäsite. Doklady Akademii Nauk SSSR. 159: 93-95 (translation).
21. Shumilova TG, Mayer E, Isaenko SI (2011) Natural monocrystalline Lonsdaleite, *Doklady Earth Sci*. 441: 1552-1554.
22. Neméth P, Garvie LAJ, Aoki T, Dubovinskaia N, Dubrovinsky L (2014) Lonsdaleite is faulted and twinned cubic diamond and does not exist as a discrete material. *Nature Communications* 5: 1-5.
23. Thomas R, Davidson P, Rericha A, Recknagel U (2022b) Discovery of stishovite in the prismatine-bearing granulite from Waldheim, Germany: A possible role of supercritical fluids of ultrahigh-pressure origin. *Geosciences*. 12: 1-15.
24. Nestola F, Korolev N, Kopylova M, Rotiroti N, Pearson DG, et al. (2018) $CaSiO_3$ perovskite in diamond indicates the recycling of oceanic crust into the lower mantle. *Nature, Letter*. 555: 237-241.
25. Wu BR (2007) Structural and vibrational properties of the 6H diamond: First-principles study. *Diamond and Related Materials*. 16: 21-28.
26. Zaitsev AM (2001) Optical Properties of Diamond - A Data Handbook. *Springer*.
27. Beyssac O, Coffee B, Chopin C, Rouzaud JN (2002) Raman spectra of carbonaceous material in metasediments: a new geothermometer. *J metamorphic Geol* 20: 859-871.
28. Frezzotti ML /2019) Diamond growth from organic compounds in hydrous fluids deep within the Earth. *Nature Communications*. 10: 1-8.
29. Gogotsi YG, Kailer A, Nickel KG (1998) Pressure-induced phase transformations in diamond. *Journal of Applied Physics*. 84: 1299-1304.
30. Meinel G (2022) Betrachtungen zum irreversiblen Verlauf der Erdgeschichte: Ein Versuch zur Beschränkung des aktualistischen Prinzips in der Geologie auf nicht von der geologischen Entwicklung abhängige Vorgänge. Berlin und Jena. Pg: 231.
31. Thomas R (2024b) Rhomboedric cassiterite as inclusions in tetragonal cassiterite from Slavkovsky les -North Bohemia. *Geol Earth Mar Sci* 6: 1-6.
32. Thomas R (2023b) Grow of SiC whisker in beryl by a natural supercritical VLS process. *Aspects in Mining and Mineral Science*. 11: 1292-1297.

Citation:

Thomas R, Leh M (2024) The Formation of Some Quartz Veins in the Lusatian Massif, E-Germany by Supercritical Fluids/Melts Bearing Lonsdaleite and Diamond and Comparison with Other Similar Formations in Middle-Saxonian and Thuringian/E-Germany. *Geol Earth Mar Sci* Volume 6(6): 1-7.